JHEP 1708 (2017) 055

Test of lepton universality with $B^0 \to K^{*0} l^+ l^-$ decays

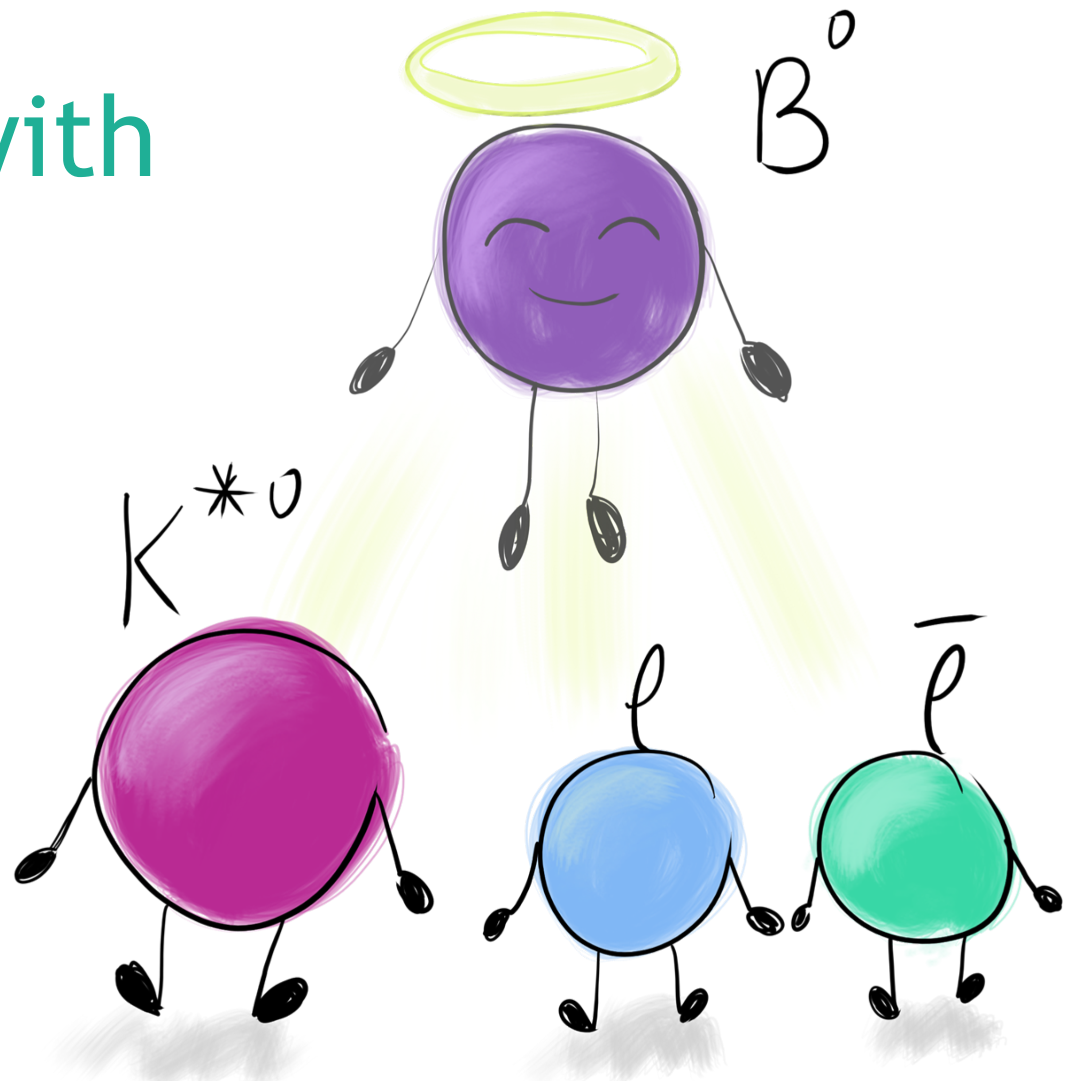

Flavour Physics
AEPSHEP2018
September 23rd, 2018, Quy Nhon, Vietnam

M. Adersberger, S. Chatterjee, E. Gabriel, J. Ghosh, S. Gu, D. Kalra, E. Kozyrev, P. Maji, T. Mkrtchyan, M. Mubasher, E. Nibigira, L. Pascual, S. Roy, N. Septain, F. Vardag, N. Yamaguchi, T. Zakareishvili, V. Zhukova

Motivation - I

- EW interactions [SU(2)x U(1)] described by Yang-Mills theory, requirement of gauge invariance→universal lepton couplings

$$R_H = \frac{\int \frac{d\Gamma(B\to H\mu^+\mu^-)dq^2)}{dq^2}}{\int \frac{d\Gamma(B\to He^+e^-)dq^2)}{dq^2}} \approx 1$$

Tests of Lepton Universality (LU)

Hints of non-universality previously observed

- BaBar, Belle: R_K =1 within 20-50% precision [1]
- LHCb: R_K with 12% precision, 2.6σ lower than SM [2]
- BaBar, Belle, LHCb: LU-violation in $B \to D^* l\nu$ [3]
- LHCb: rare b→s decays $(B \to K^*\mu^+\mu^-, B_s^0 \to \phi\mu^+\mu^-, \Lambda_b^0 \to \Lambda\mu^+\mu^-)$ Lower differential branching fractions than Standard Model (SM). [4,5,6]

Motivation - II

Flavour changing neutral currents (FCNC) *forbidden* at *tree level* in SM
FCNC allowed at *loop level*→suppressed→ sensitivity to NP

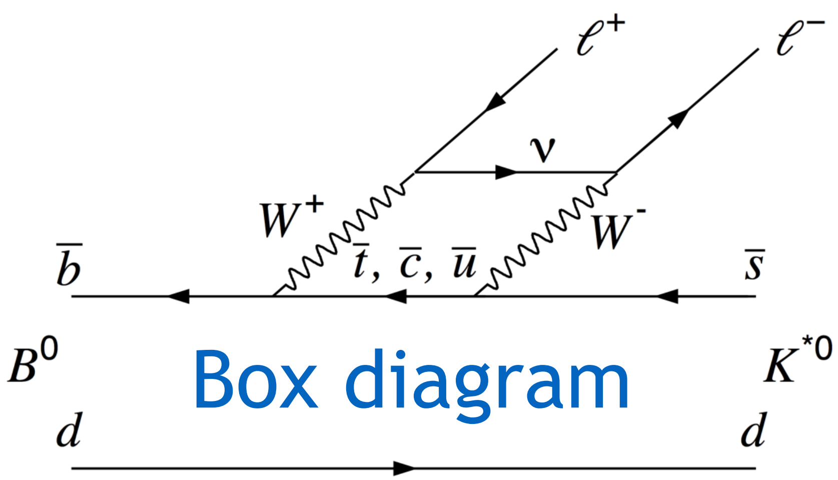

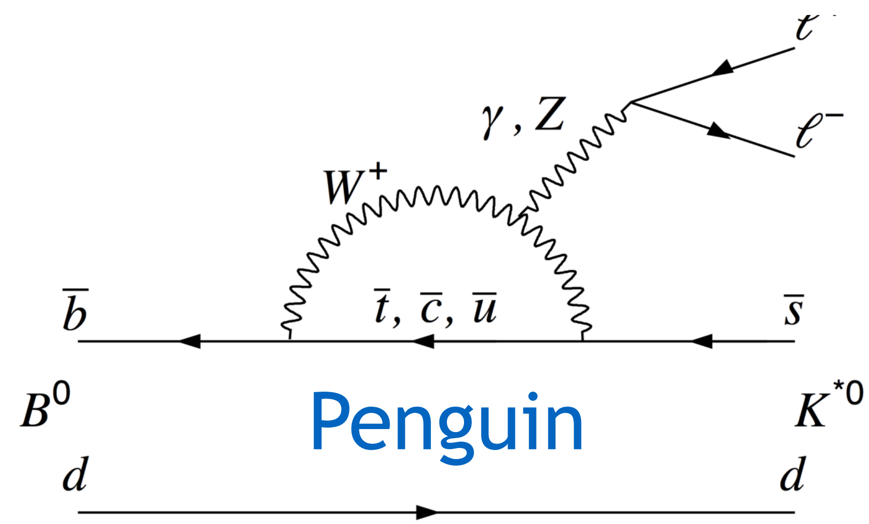

SM scenario

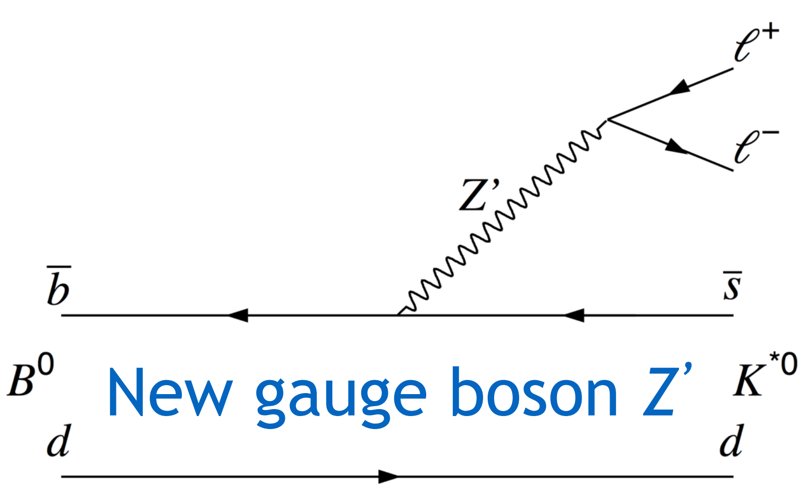

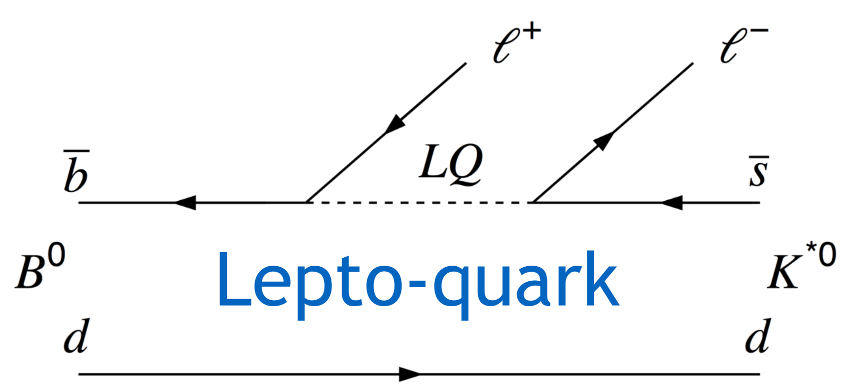

NP scenario

Phys. Rev. D **88**, 074002, (2013)

Phys. Rev. D **94**, 115021,(2016)

Motivation - III

Reduces systematic uncertainties

- Double ratio of branching fractions

Non-resonant mode

$$R_{K^{*0}} = \frac{\mathcal{B}(B^0 \to K^{*0}\mu^+\mu^-)}{\mathcal{B}\left(B^0 \to K^{*0}J/\psi(\to \mu^+\mu^-)\right)} \Big/ \frac{\mathcal{B}(B^0 \to K^{*0}e^+e^-)}{\mathcal{B}\left(B^0 \to K^{*0}J/\psi(\to e^+e^-)\right)}$$

Resonant mode

- Analysis performed in two bins of dilepton invariant mass:

low q^2 – bin	central q^2 – bin
0.045 - 1.1 GeV^2	1.1 - 6.0 GeV^2

dimuon kinematic threshold

$\phi(1020)$ resonance in low-q^2 bin

reduce contamination from J/ψ

The LHCb detector

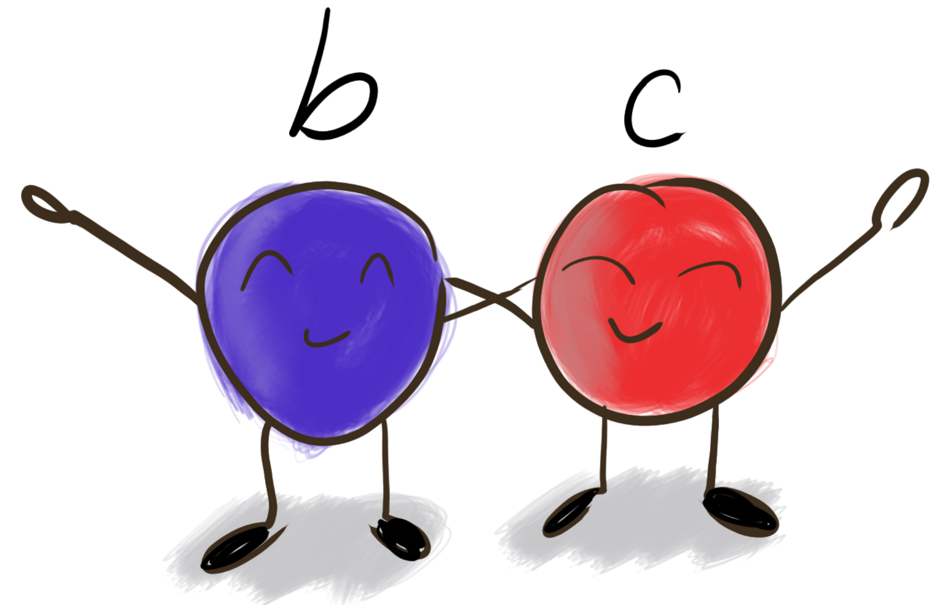

Aimed at studying physics involving b (and c) quarks

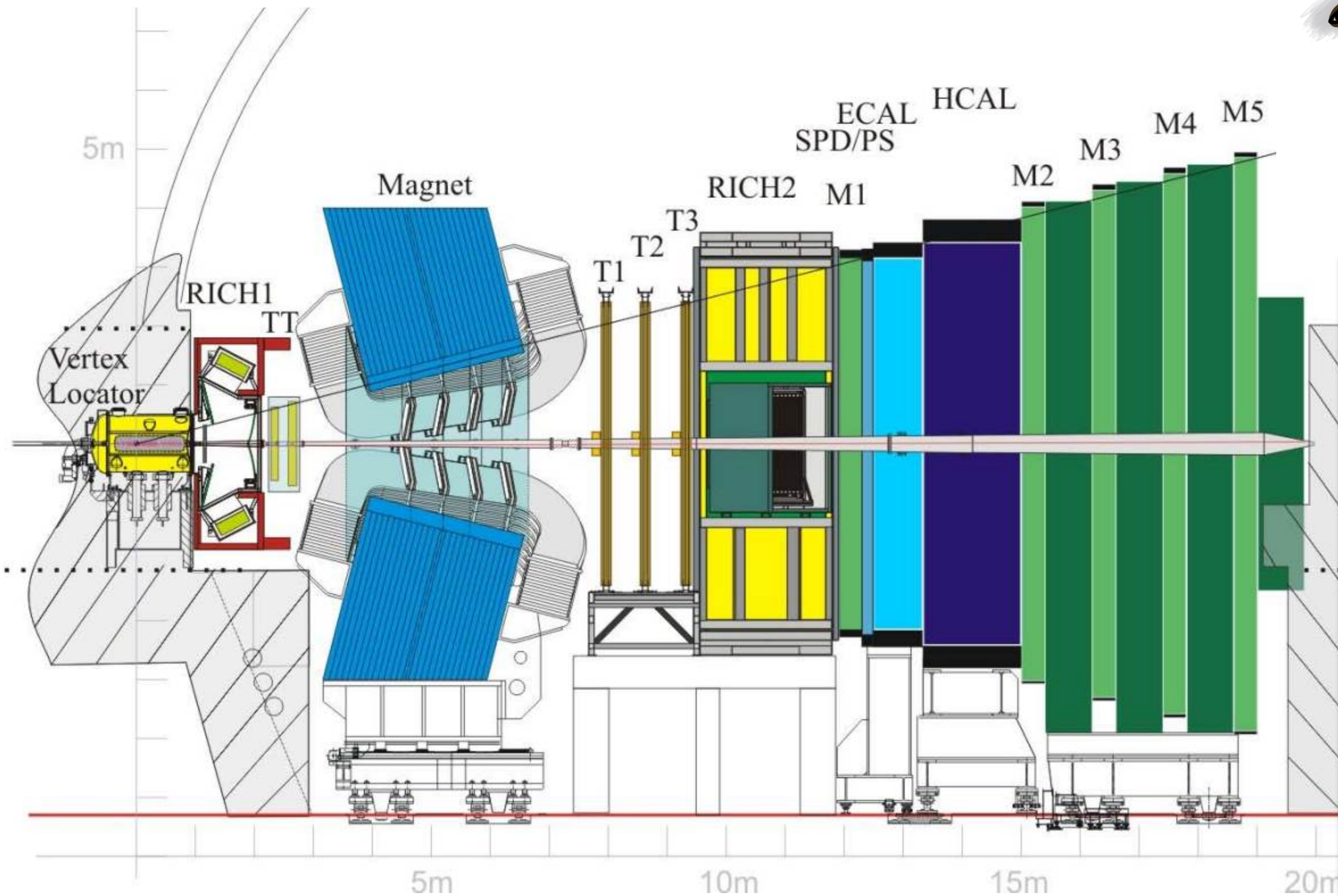

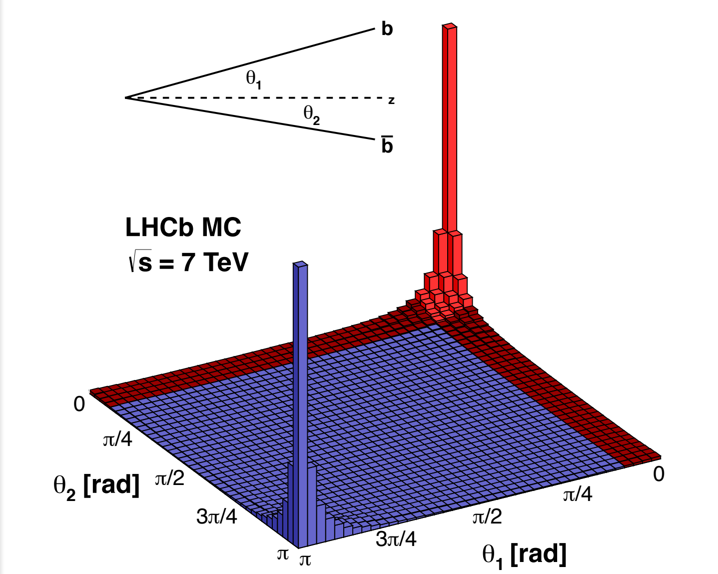

Forward arm spectrometer

Pseudorapidity $2 < \eta < 5$

Electron Reconstruction

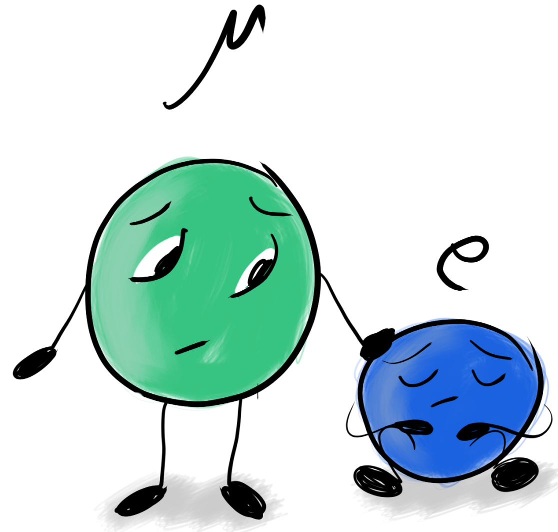

Decays involving muons and electrons require different treatment at LHCb.

- Electrons emit much larger amounts of bremsstrahlung
- Degradation of momentum resolution
- Two types of bremsstrahlung: *upstream* and *downstream* of the magnet

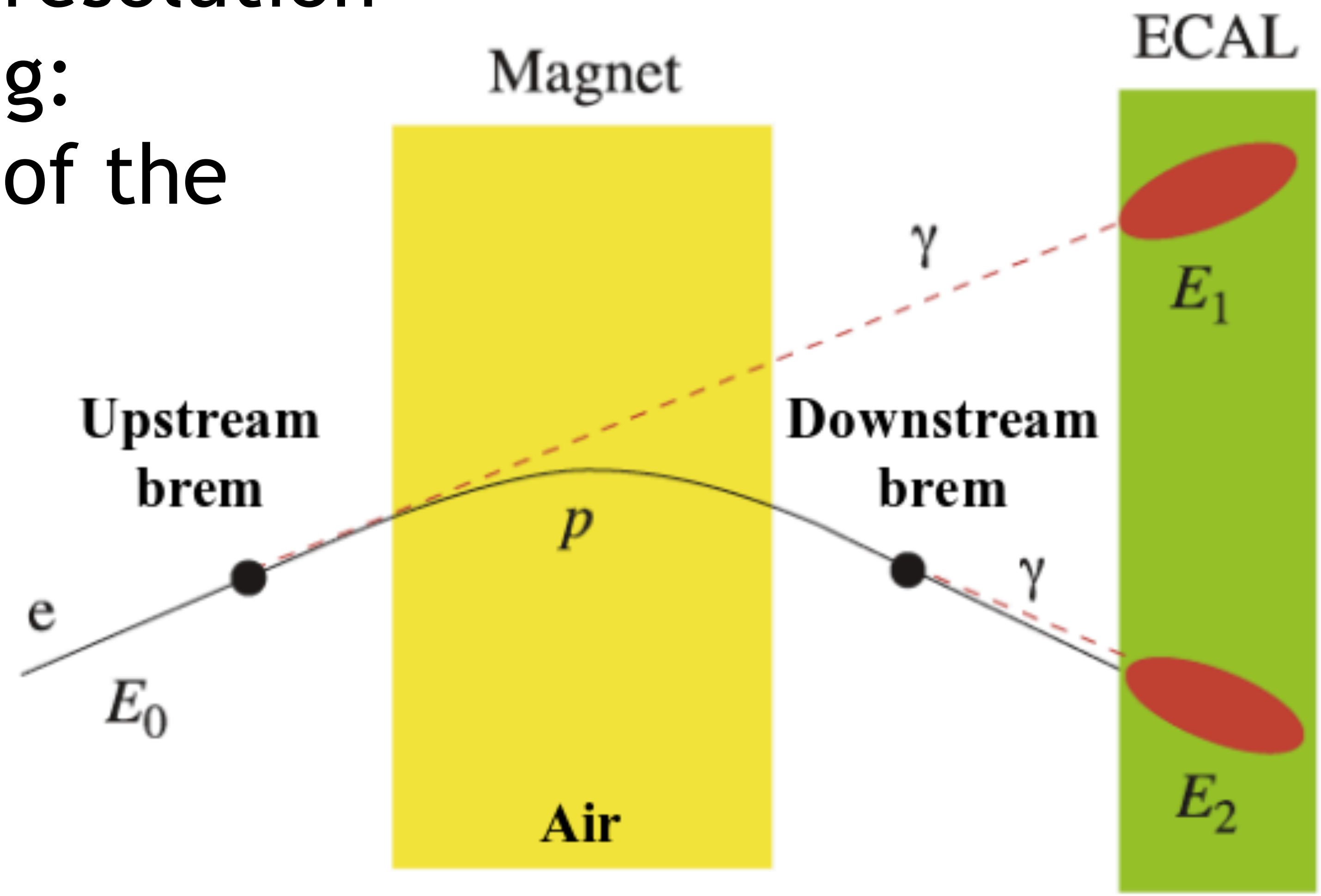

A bremsstrahlung recovery procedure is required for electrons.

Selection and Backgrounds

dilepton invariant mass (squared)

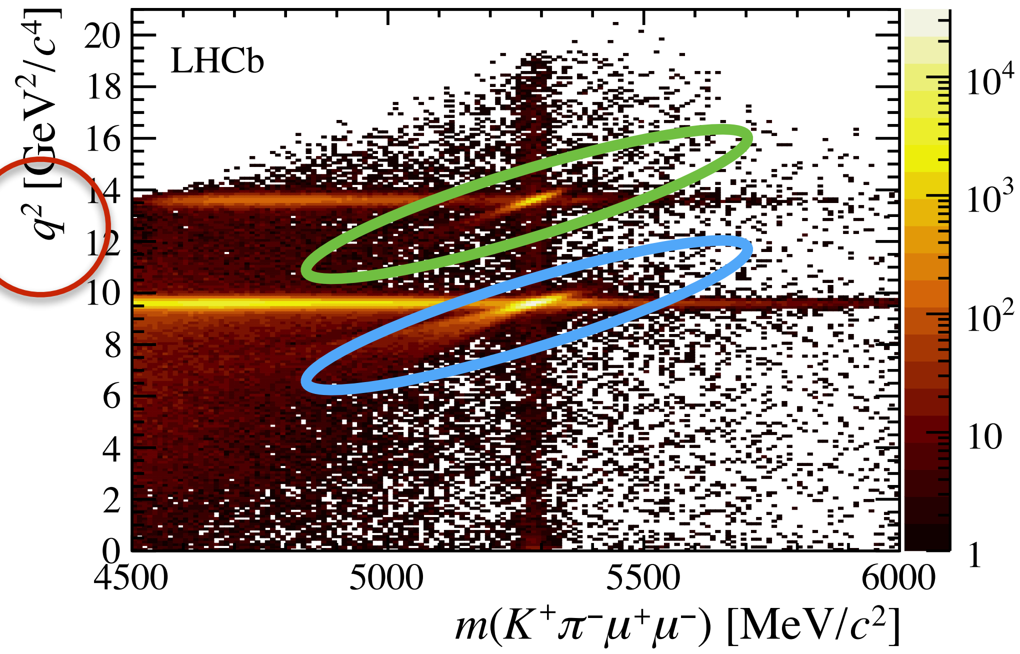

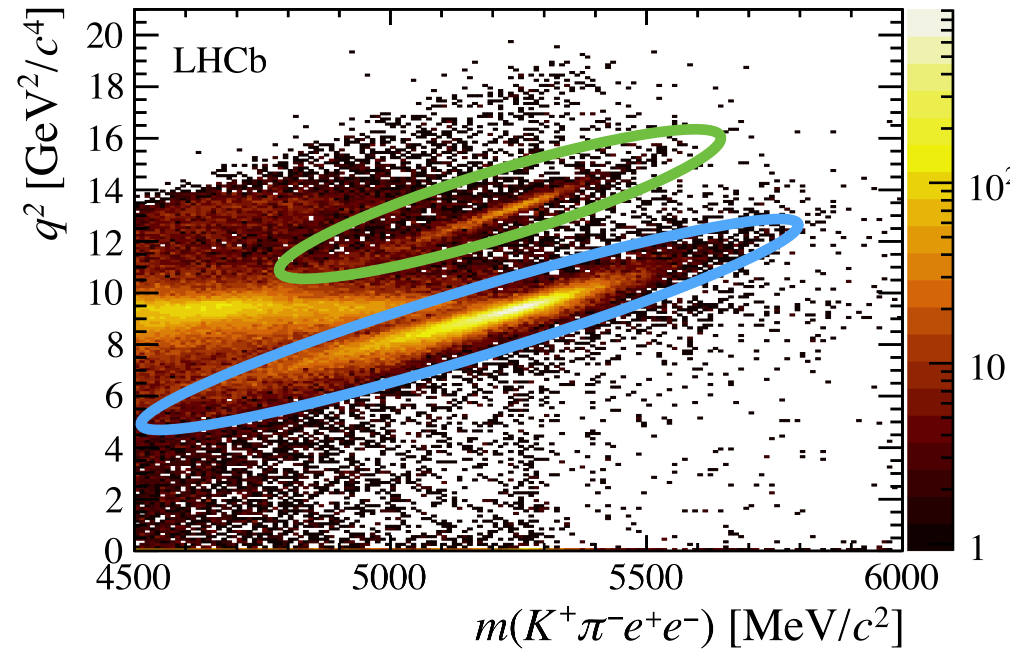

Selection consists of:

- Trigger lines
- Cut-based selection
- Multivariate neural network

- **m(B^0)** ≈ 5.3 GeV/c^2
- **m(J/ψ)** ≈ 3.1 GeV/c^2
  → **<q^2>** ≈ 9.6 GeV^2/c^4
- **m(ψ(2s))** ≈ 3.7 GeV/c^2
  ⟶ **<q^2>** ≈ 13.7 GeV^2/c^4

Final signal regions

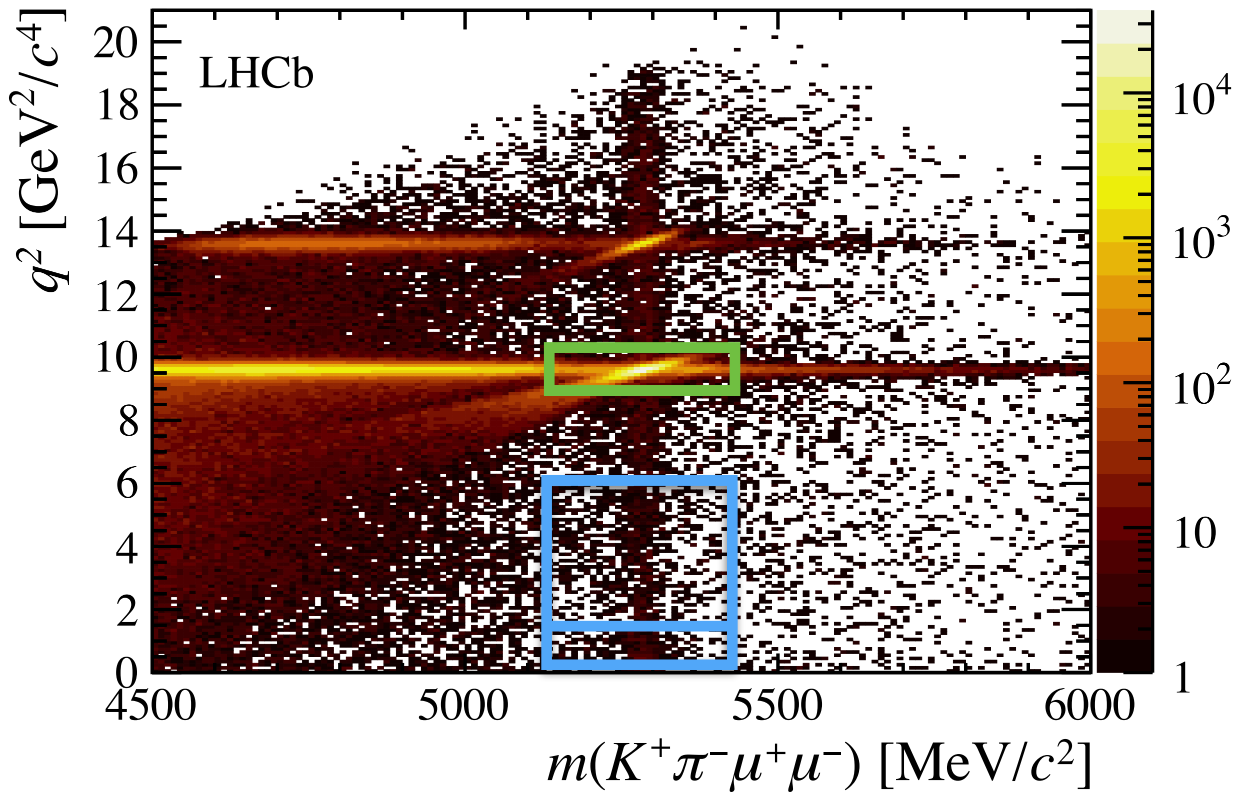

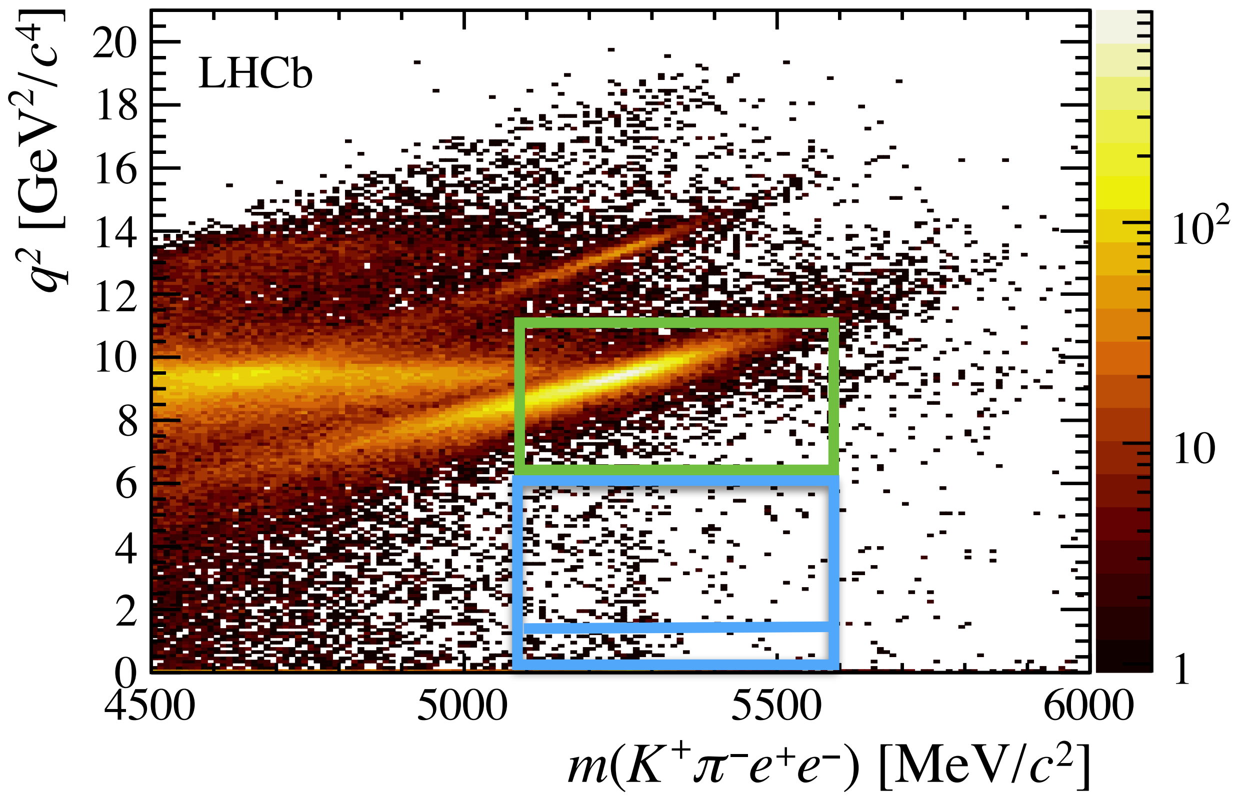

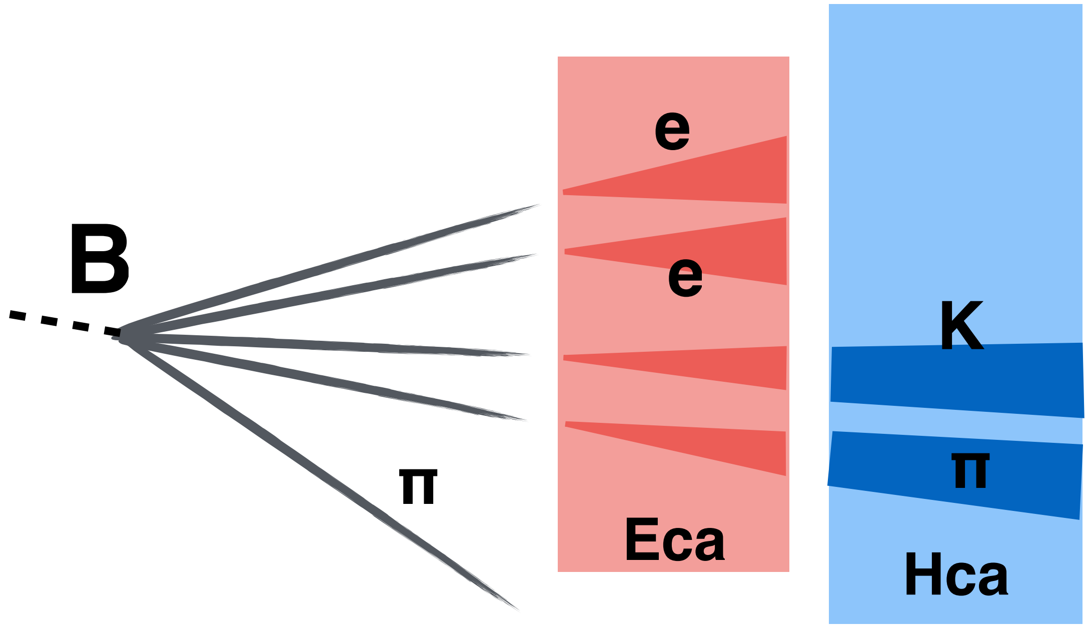

green: $B^0 \to K^+\pi^- J/\psi$

blue: $B^0 \to K^+\pi^- l^+ l^-$

- Further backgrounds smaller and/or suppressible
- Bremsstrahlung degrades electrons momentum resolution

Fit results - μμ

- Fit to simulation to extract initial parameters
- Fit the data allowing some parameters to vary
- Simultaneous fit to resonant and non-resonant modes with some shared parameters

signal model

- Hypatia function

background model

- combinatorial: exponential
- resonant partially reconstructed backgrounds from simulation

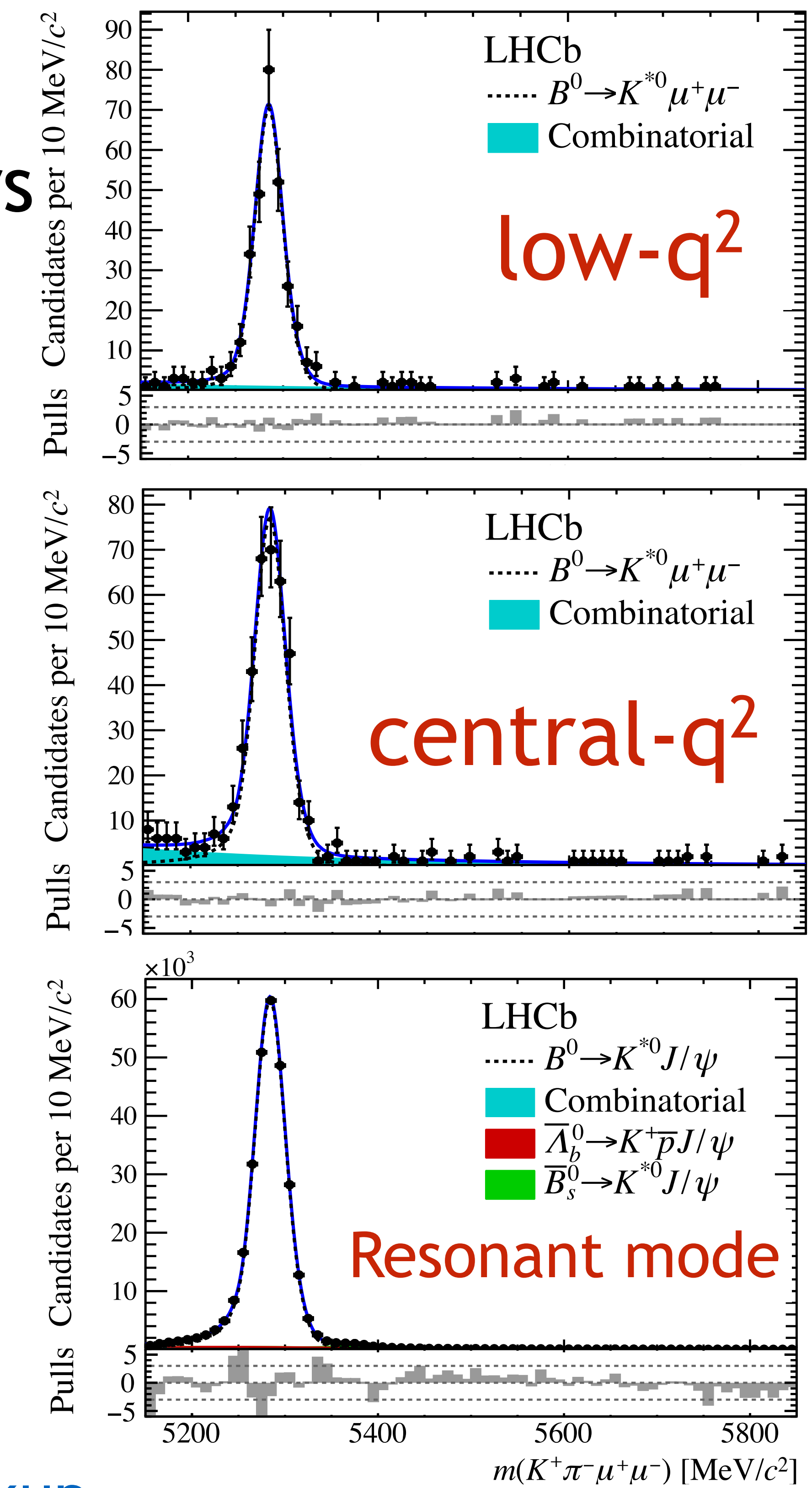

Slightly more complicated fit procedure for ee - see backup

Statistics and Systematics

	$B^0 \to K^{*0}\ell^+\ell^-$		$B^0 \to K^{*0}J/\psi\,(\to \ell^+\ell^-)$
	low- q^2	central- q^2	
$\mu^+\mu^-$	$285\,^{+\,18}_{-\,18}$	$353\,^{+\,21}_{-\,21}$	$274416\,^{+\,602}_{-\,654}$
e^+e^- (L0E)	$55\,^{+\,9}_{-\,8}$	$67\,^{+\,10}_{-\,10}$	$43468\,^{+\,222}_{-\,221}$
e^+e^- (L0H)	$13\,^{+\,5}_{-\,5}$	$19\,^{+\,6}_{-\,5}$	$3388\,^{+\,62}_{-\,61}$
e^+e^- (L0I)	$21\,^{+\,5}_{-\,4}$	$25\,^{+\,7}_{-\,6}$	$11505\,^{+\,115}_{-\,114}$

- Fit yields (purely statistics errors) taken as direct input to R(K*)

- Main *systematic error* comes from corrections to the simulation
  Total systematic error is 4-6% (6-8%) in low(central)-q^2 bin
- Many experimental systematic effects cancel due to double ratio with resonant mode.

- *Precision of the measurement driven by the statistical error* on the electron channel yields (~15%)

Results

Theoretical predictions

	low- q^2	central- q^2
$R_{K^{*0}}$	$0.66\,^{+\,0.11}_{-\,0.07} \pm 0.03$	$0.69\,^{+\,0.11}_{-\,0.07} \pm 0.05$

Experimental results

	$R^{\mathrm{SM}}_{K^{*0}}$	References
low- q^2	0.906 ± 0.028	BIP[26]
	0.922 ± 0.022	CDHMV[27,28,29]
	$0.919\,^{+\,0.004}_{-\,0.003}$	EOS[30,31]
	0.925 ± 0.004	flav.io[33,34,35]
	$0.920\,^{+\,0.007}_{-\,0.006}$	JC[36]
central- q^2	1.000 ± 0.010	BIP[26]
	1.000 ± 0.006	CDHMV[27,28,29]
	$0.9968\,^{+\,0.0005}_{-\,0.0004}$	EOS[30,31]
	0.9964 ± 0.005	flav.io[33,34,35]
	0.996 ± 0.002	JC[36]

Results are compatible with SM predictions at:

- 2.1-2.3 σ in the low-q^2 region
- 2.4-2.5 σ in the central-q^2 region

This is the most precise experimental measurement of $R(K^{*0})$ to date.
The analysis is based on the full Run-I sample of LHCb data taken between 2010-2012 of 3 fb^{-1}.

Taken from: CERN-LHCC-2017-003

Future Prospects

Based on a specific New Physics model outlined in arXiv:1610.08761

Prediction from a model based on two different effective field operators.

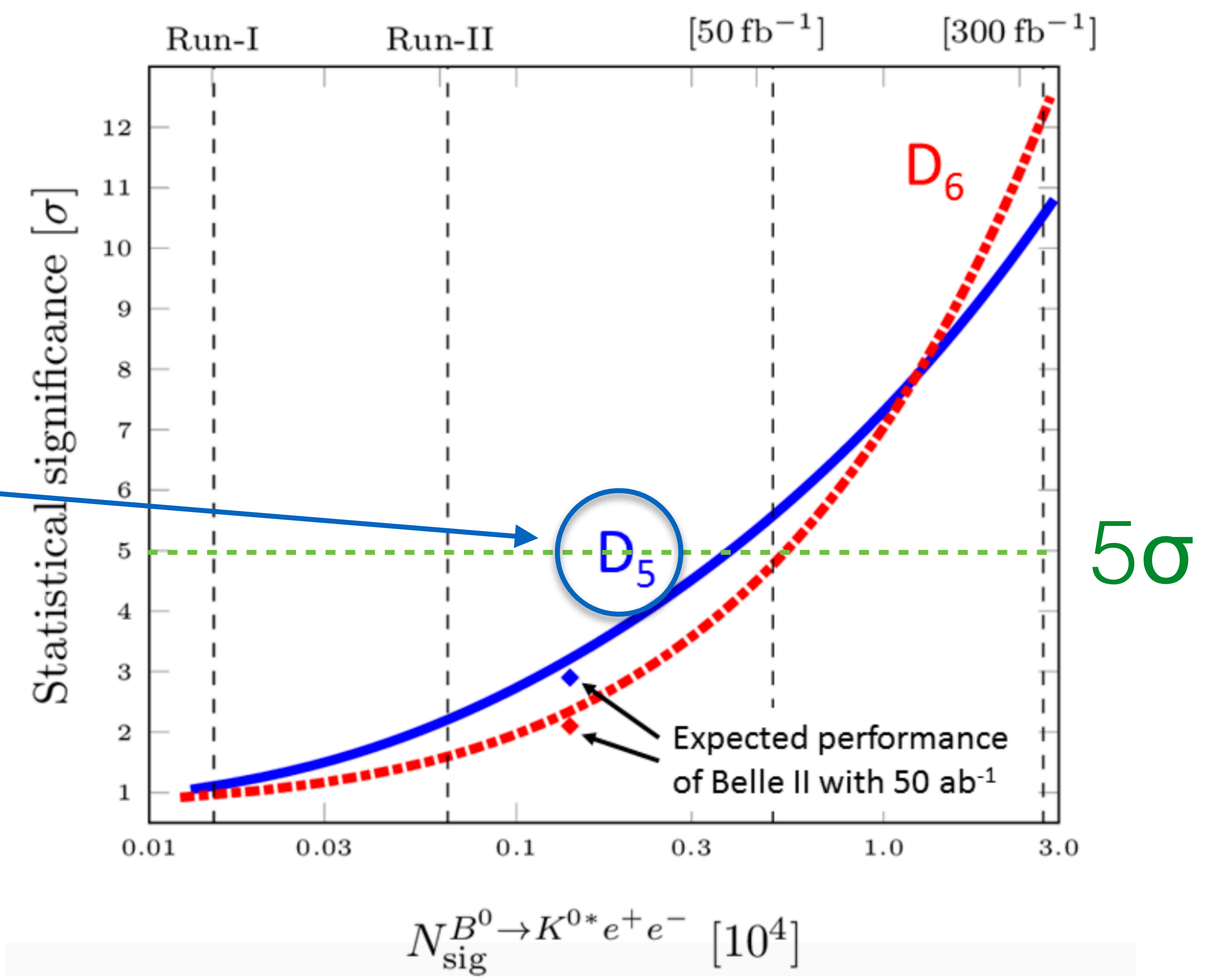

Increasing the signal yield for the ee final state will greatly improve the precision by reducing the statistical error.

Very exciting future for LFU lies ahead!

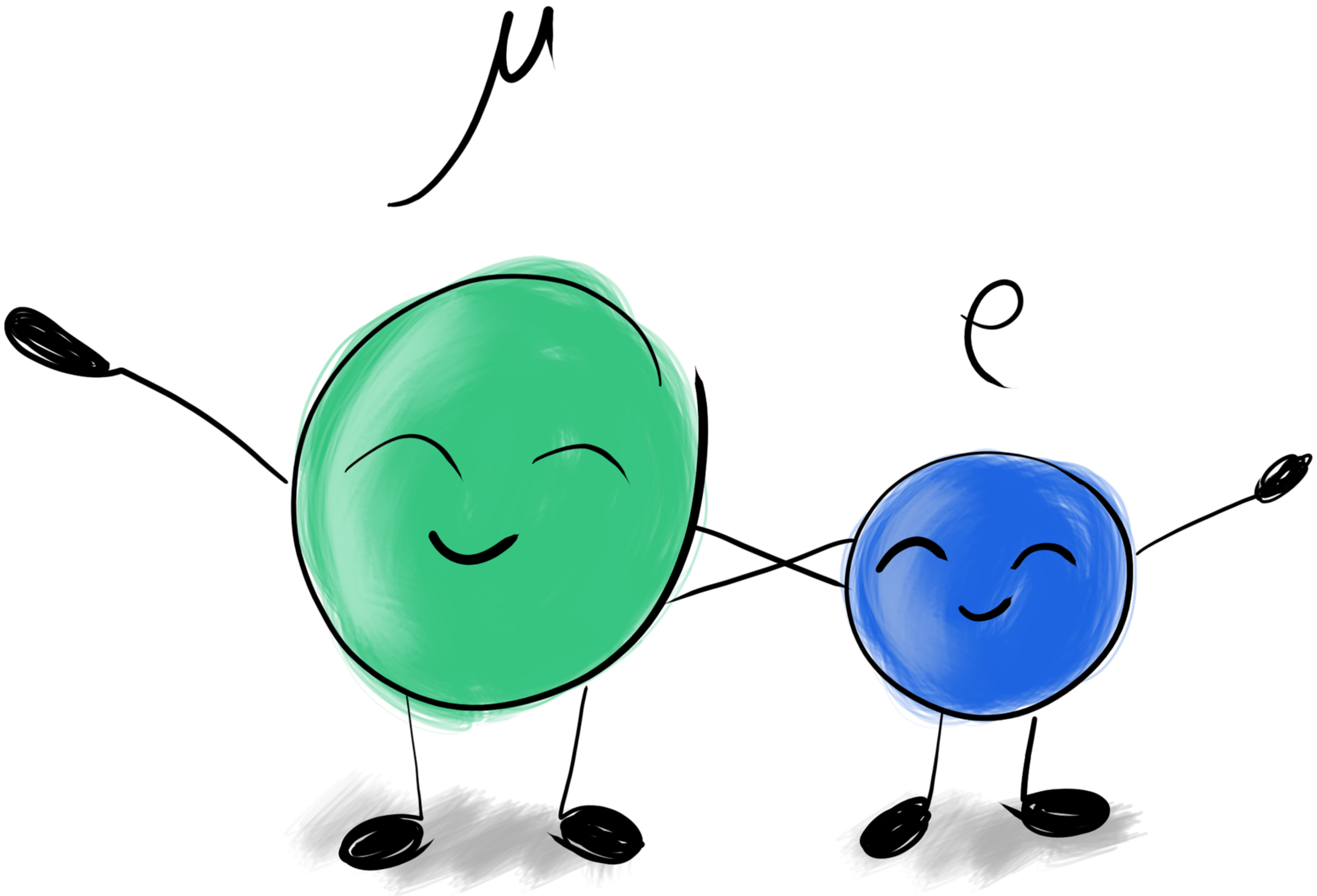

References

[1] PRD **86** (2012) 032012, PRL **103** (2009) 171801
[2] PRL **113** (2014) 151601
[3] PRD **79** (2009) 012002; PRD **92** (2015) 072014;
PRL**115** (2015) 111803
[4] arXiv:1606.04731
[5] JHEP 09 (2015) 179
[6] JHEP 06 (2015) 115
[7] JHEP 01 (2009) 019

Backup Slides

Lepto-quarks (LQ)

- Lepto-quarks are hypothetical particles that allow quarks and leptons of a given generation to interact.
- They are color-triplet bosons that carry both lepton and baryon number.

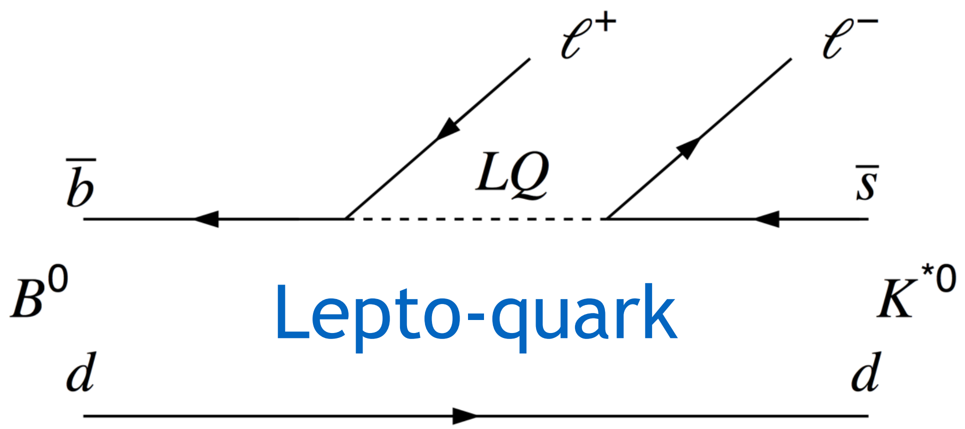

Simulation Corrections

Simulation corrections account for the largest source of systematic uncertainty in the analysis.

Corrections to the simulation:

- PID performance - response of each particle tuned to dedicated calibration samples
- Charged track multiplicity - accounted for using the well-modelled $B^0 \to K^{*0} J/\psi(\to \mu^+\mu^-)$ decay.
- Trigger response tuned using resonant decay
- Residual data/MC differences tuned using $B^0 \to K^{*0} J/\psi(\to ll)$

Electron Reconstruction

Electrons emit a much larger amount of bremsstrahlung than muons – results in a significant degradation of the momentum resolution.

- **Downstream beam**: radiation occurs downstream of the dipole magnet, the photon energy is deposited in the same calorimeter cell as that of the lepton, and the momentum of the electron is correctly measured.
- **Upstream beam**: photons are emitted upstream of the magnet, the electron and photon deposit their energy in different calorimeter cells, and the electron momentum is evaluated after bremsstrahlung emission.

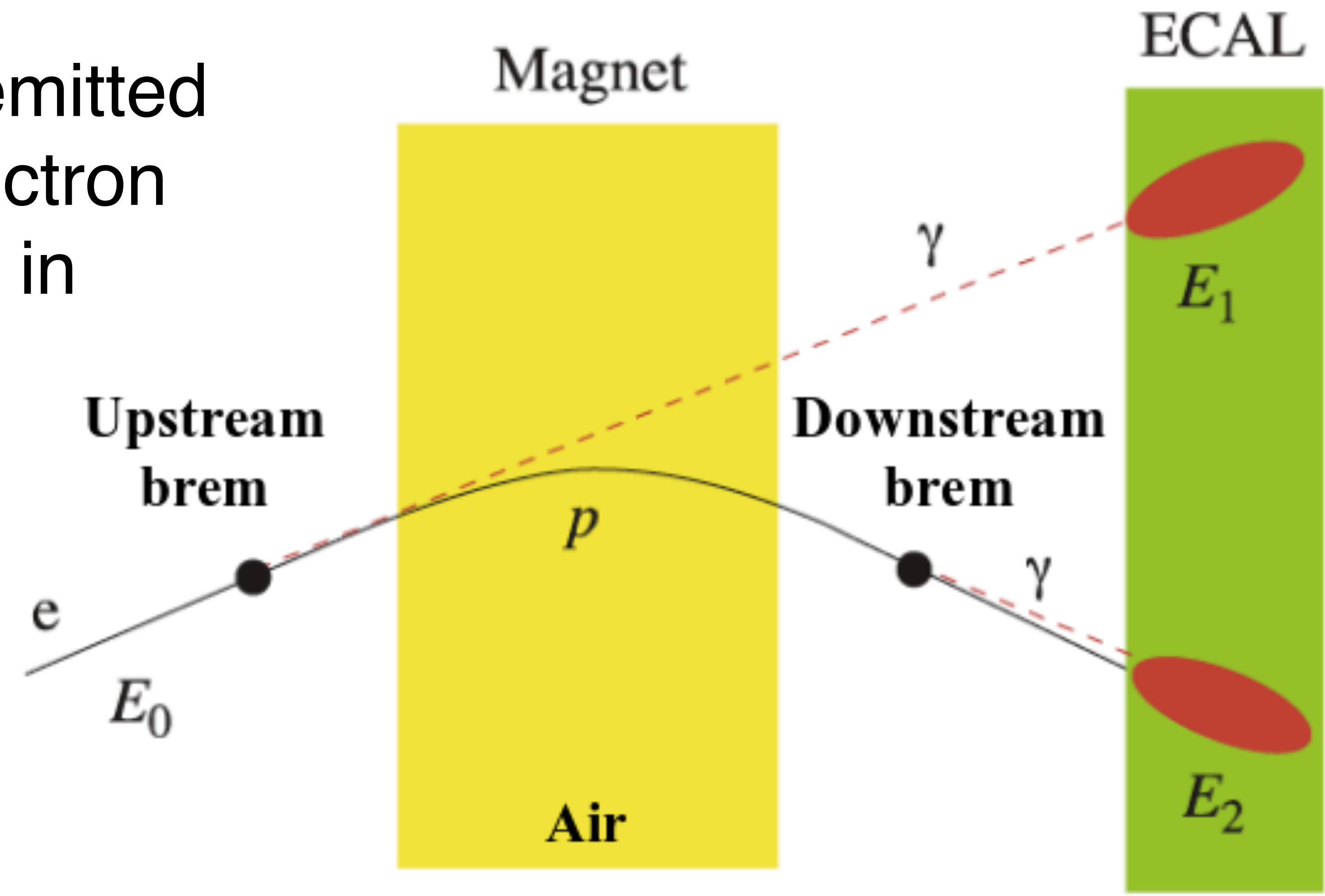

Bremsstrahlung Recovery

- Event categorised depending on the number of recovered photon clusters (i.e. energy deposits not associated with a charged track).
- These ‘photons’ are added to the electron momentum.

Limitations of this procedure:

- Energy thresholds of ‘photon’ clusters means low energy photons are disregarded
- Calorimeter acceptance and resolution
- Presence of energy clusters wrongly interpreted as a bremsstrahlung photon.

- Differences due to bremsstrahlung and the trigger response lead to a reconstruction efficiency for the resonant electron decays that is about five times smaller than for the resonant muon decays.

Fit results - ee

- Fit to simulation to extract initial parameters
- Fit the data split in trigger categories allowing some parameters to vary
- Fix bremsstrahlung fractions to simulation
- Simultaneous fit to resonant and non-resonant modes with some shared parameters
- More backgrounds to be considered in ee case.

signal model

- Gaussian + Crystal Ball

background model

- combinatorial: exponential
- resonant part-reco backgrounds from MC

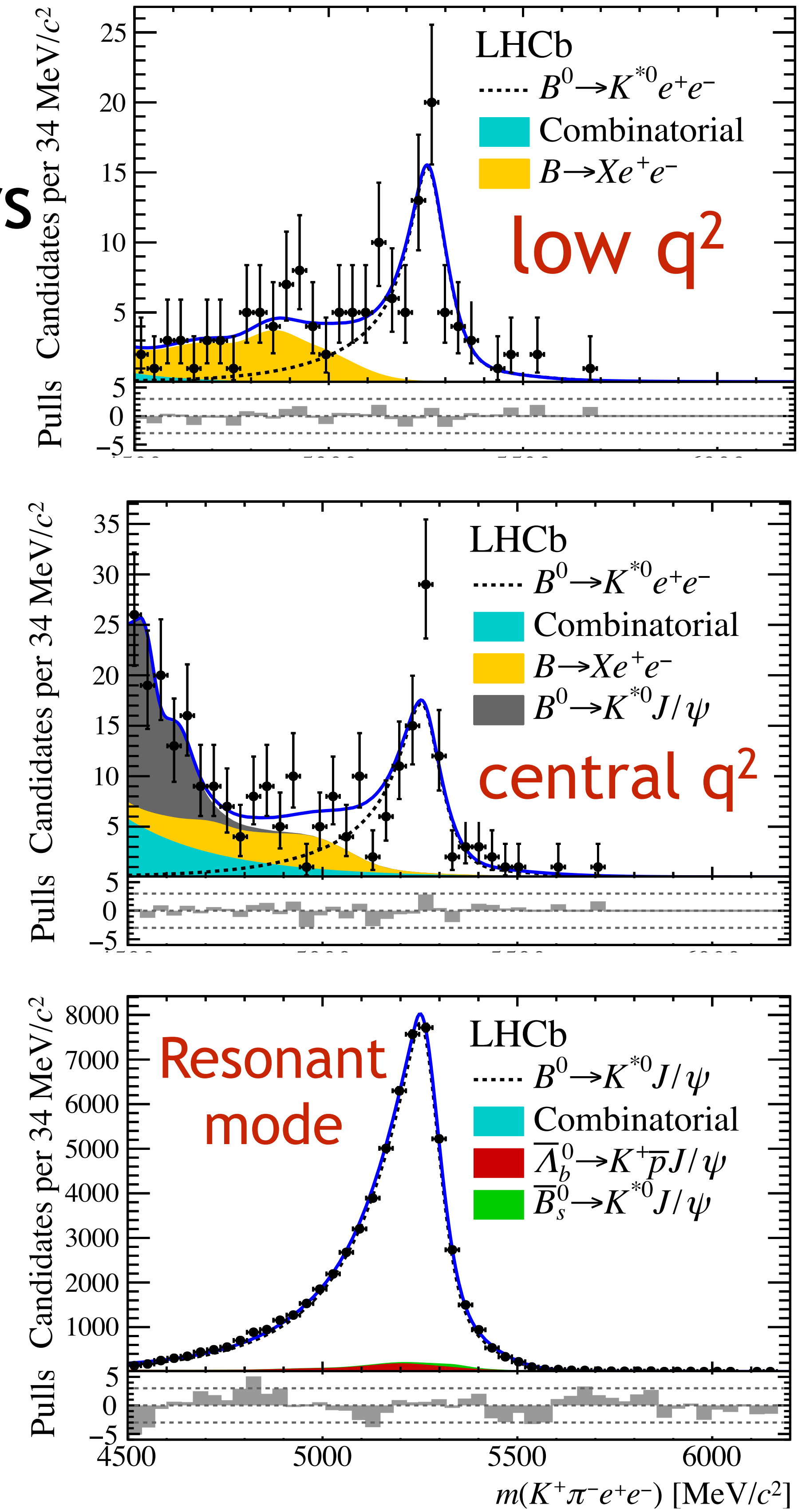

Systematics-I

	$\Delta R_{K^{*0}}/R_{K^{*0}}$ [%]					
	low- q^2			central- q^2		
Trigger category	L0E	L0H	L0I	L0E	L0H	L0I
Corrections to simulation	2.5	4.8	3.9	2.2	4.2	3.4
Trigger	0.1	1.2	0.1	0.2	0.8	0.2
PID	0.2	0.4	0.3	0.2	1.0	0.5
Kinematic selection	2.1	2.1	2.1	2.1	2.1	2.1
Residual background	–	–	–	5.0	5.0	5.0
Mass fits	1.4	2.1	2.5	2.0	0.9	1.0
Bin migration	1.0	1.0	1.0	1.6	1.6	1.6
$r_{J/\psi}$ ratio	1.6	1.4	1.7	0.7	2.1	0.7
Total	4.0	6.1	5.5	6.4	7.5	6.7

Efficiencies

- Efficiencies computed for each decay mode as the product of:

$$\varepsilon_{tot} = \varepsilon_{PID} \times \varepsilon_{detector} \times \varepsilon_{track} \times \varepsilon_{trigger} \times \varepsilon_{bkg}$$

- Different efficiencies for:
  - Each q^2 bin
  - Each electron trigger (L0E, L0H , L0I)

	$\varepsilon_{\ell^+\ell^-}/\varepsilon_{J/\psi(\ell^+\ell^-)}$	
	low-q^2	central-q^2
$\mu^+\mu^-$	0.679 ± 0.009	0.584 ± 0.006
e^+e^- (L0E)	0.539 ± 0.013	0.522 ± 0.010
e^+e^- (L0H)	2.252 ± 0.098	1.627 ± 0.066
e^+e^- (L0I)	0.789 ± 0.029	0.595 ± 0.020

- L0E q^2 independent
- L0H larger due to different requirements in the neural network classifier.
- L0I q^2 mildly dependent

Magnetic field in LHCb

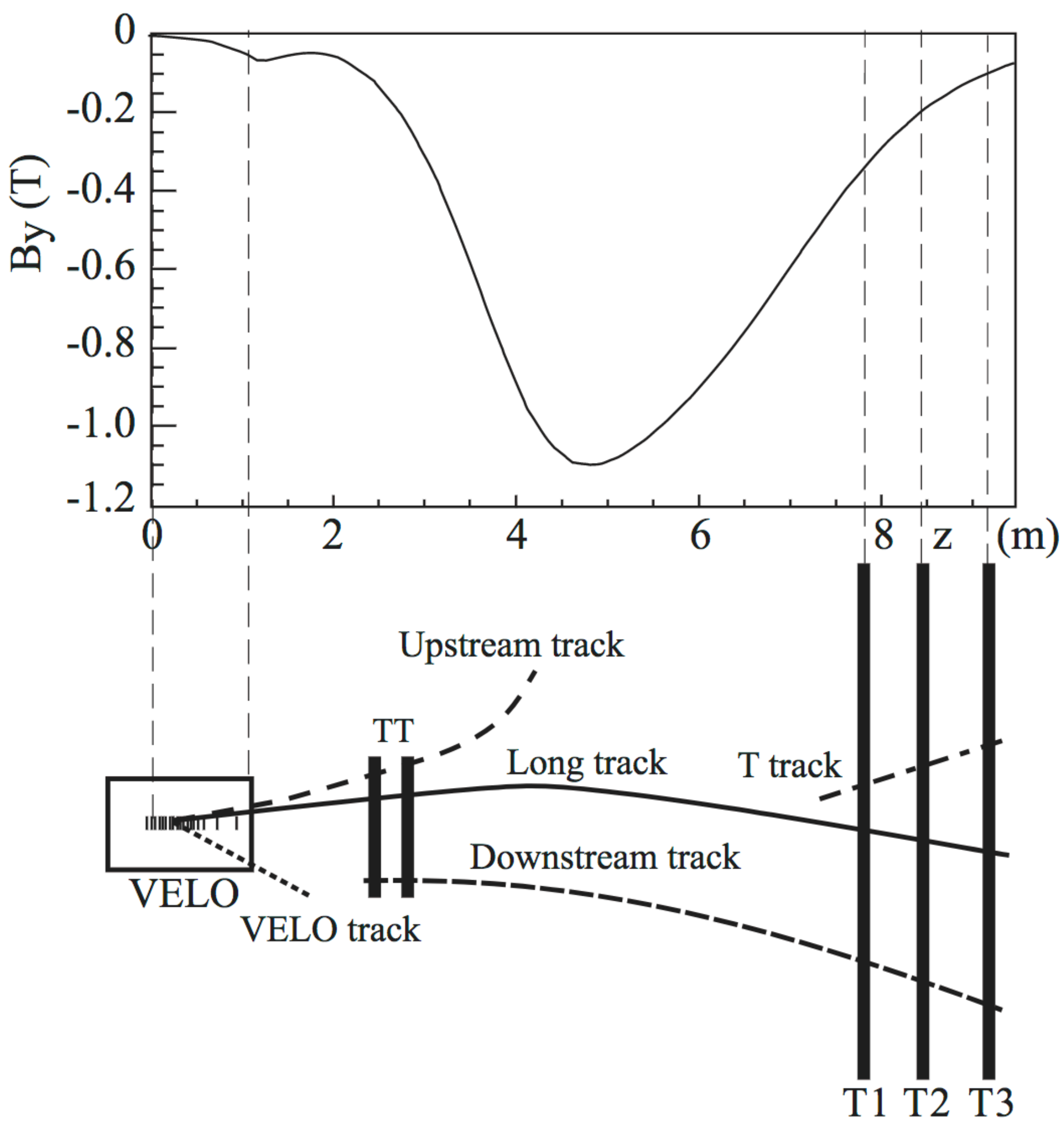

- Long tracks traverse the full tracking system and therefore they have the most precise momentum estimate.
- Downstream tracks are important for long-lived neutral particles such as K^0_S and Λ.
- Upstream tracks are low p_T particles used to understand the background (with information from the RICH1 detector)

Analysis binning

Low-q^2 region: [0.045, 1.1] GeV^2
Central-q^2 region: [1.1, 6.0] GeV^2

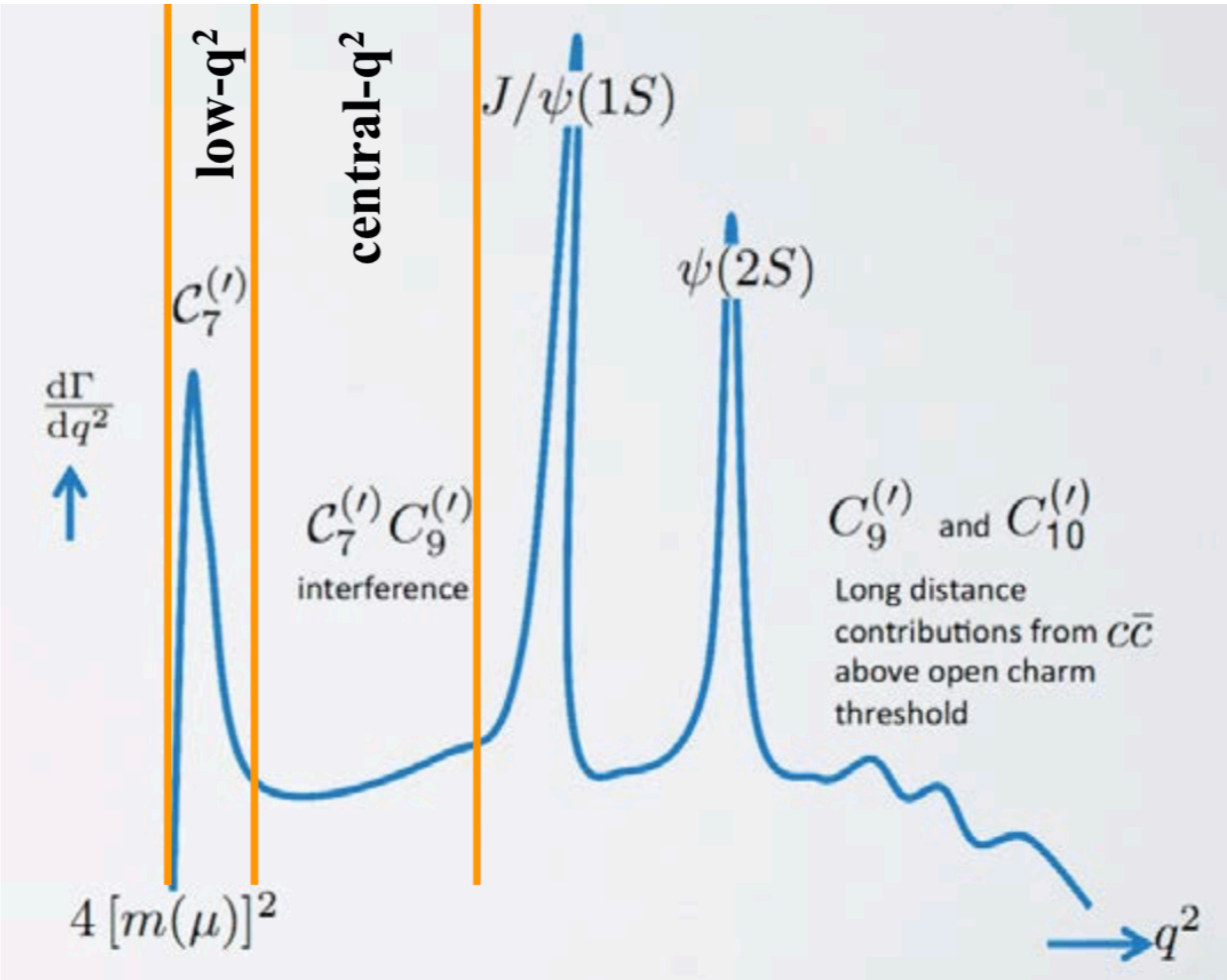

- The lower boundary of the low-q^2 region corresponds roughly with the dimuon kinematic threshold.
- The boundary at 1.1 GeV^2 is chosen such that $\phi(1020) \to l^+l^-$ is included in the low-q^2 region.
- The upper boundary of the central-q^2 region is chosen to reduce the contamination from the radiative tail of the J/Ψ resonance.

CrystalBall p.d.f.

$$p(m) \propto \begin{cases} e^{-\frac{1}{2}\left(\frac{m-\mu}{\sigma}\right)^2} & \text{, if } \frac{m-\mu}{\sigma} > -a \\ A\left(B - \frac{m-\mu}{\sigma}\right)^n & \text{, otherwise} \end{cases}$$

- The CrystalBall distribution is commonly used to describe mass peaks with a radiative tail to lower energies.
- Gaussian core to account for the detector resolution.
- A and B are constants to ensure the continuity of the distribution.

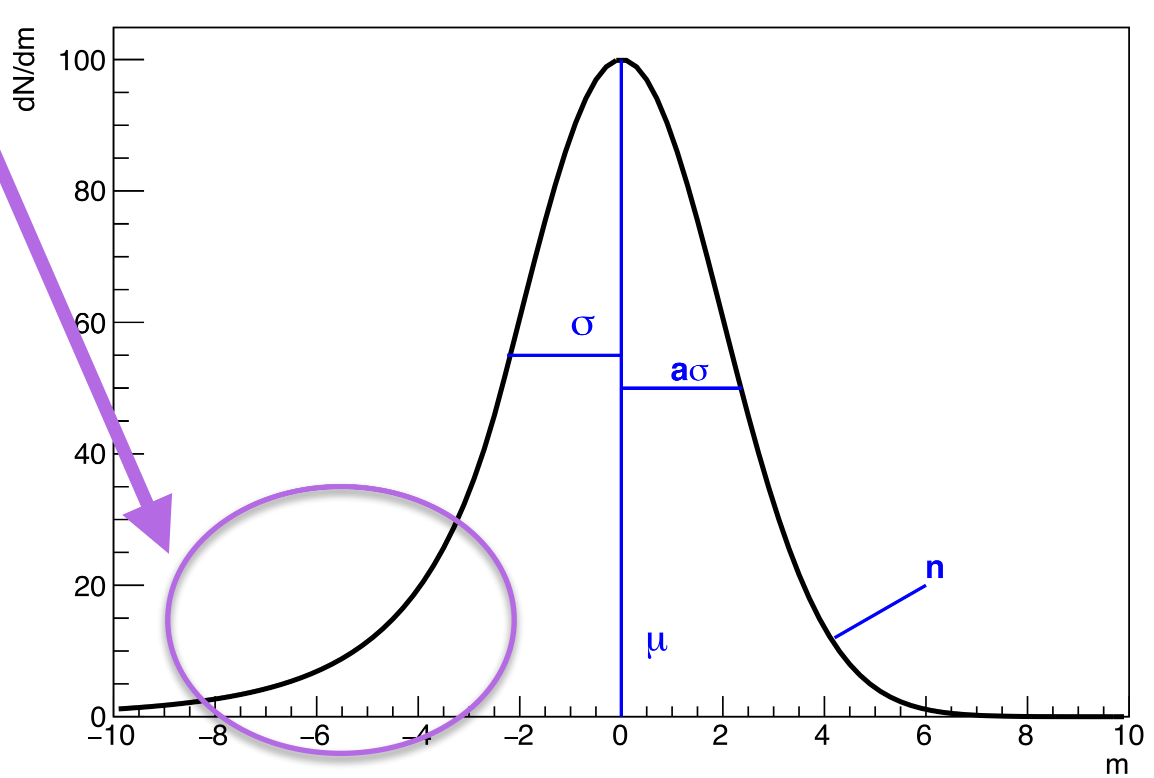

Hypatia p.d.f.

$$p(m) \propto \begin{cases} e^{-\frac{1}{2}\left(\frac{m-\mu}{\sigma}\right)^2} & \text{, if } \frac{m-\mu}{\sigma} > -a \\ A\left(B - \frac{m-\mu}{\sigma}\right)^n & \text{, otherwise} \end{cases}$$

$$G(m,\mu,\sigma,\lambda,\zeta,\beta) \propto$$

$$\left((m-\mu)^2 + A_\lambda^2(\zeta)\sigma^2\right)^{\frac{1}{2}\lambda-\frac{1}{4}} e^{\beta(m-\mu)} K_{\lambda-\frac{1}{2}}\left(\zeta\sqrt{1+\left(\frac{m-\mu}{A_\lambda(\zeta)\sigma}\right)^2}\right)$$

$$I(m,\mu,\sigma,\lambda,\zeta,\beta,a,n) \propto$$

$$\begin{cases} \left((m-\mu)^2 + A_\lambda^2(\zeta)\sigma^2\right)^{\frac{1}{2}\lambda-\frac{1}{4}} e^{\beta(m-\mu)} K_{\lambda-\frac{1}{2}}\left(\zeta\sqrt{1+\left(\frac{m-\mu}{A_\lambda(\zeta)\sigma}\right)^2}\right) & \text{, if } \frac{m-\mu}{\sigma} > -a \\ \frac{G(\mu-a\sigma,\mu,\sigma,\lambda,\zeta,\beta)}{\left(1-m/\left(n\frac{G(\mu-a\sigma,\mu,\sigma,\lambda,\zeta,\beta)}{G'(\mu-a\sigma,\mu,\sigma,\lambda,\zeta,\beta)}-a\sigma\right)\right)^n} & \text{, otherwise} \end{cases}$$

- Hypatia distribution is a generalised CrystalBall distribution suited for analysis in which the uncertainties can vary in a per-event basis.

Result

Result consistent among different trigger categories as well as the combination of the triggers.

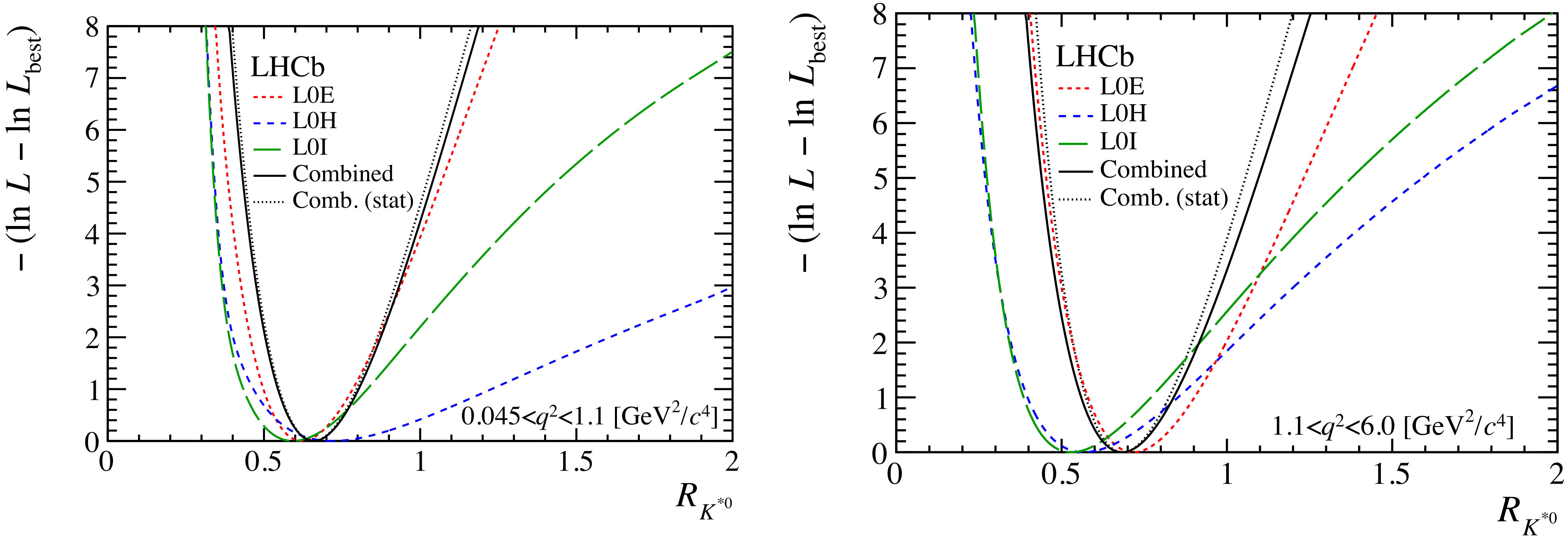

LU test

$\mathcal{O}_{9(9')} = [\bar{s}\gamma_\mu P_{L(R)} b][\bar{l}\gamma^\mu l]$ $\mathcal{O}_{10(10')} = [\bar{s}\gamma_\mu P_{L(R)} b][\bar{l}\gamma^\mu \gamma_5 l]$

- LU tests can be performed through the study of angular observables of the decay $B^0 \to K^* l^+ l^-$
- In the considered NP contributions ([7]), the CP-averaged angular observables are:

$$S_i(q^2) \equiv \frac{4}{3} \frac{J_i(q^2) + \bar{J}_i(q^2)}{d\Gamma/dq^2 + \overline{d\Gamma}/dq^2}$$

$$D_i(q^2) \equiv \frac{d\mathcal{B}^{(e)}}{dq^2} S_i^{(e)}(q^2) - \frac{d\mathcal{B}^{(\mu)}}{dq^2} S_i^{(\mu)}(q^2)$$

where:

- J_i are angular coefficients (next slide)
- $\mathcal{B}^{(l)}$ are the branching ratios of each lepton
- Barred quantities stand for CP-conjugation.

Deviations from the SM prediction would imply LU violation

Decay distribution of $\overline{B}^0 \to \overline{K}^{*0}(\to K^-\pi^+)l^+l^-$

$$\frac{d^4\Gamma}{dq^2\, d\cos\theta_l\, d\cos\theta_{K^*}\, d\phi} = \frac{9}{32\pi} I(q^2, \theta_l, \theta_{K^*}, \phi)\,, \tag{3.9}$$

where

$$\begin{aligned} I(q^2, \theta_l, \theta_{K^*}, \phi) = {} & I_1^s \sin^2\theta_{K^*} + I_1^c \cos^2\theta_{K^*} + (I_2^s \sin^2\theta_{K^*} + I_2^c \cos^2\theta_{K^*}) \cos 2\theta_l \\ & + I_3 \sin^2\theta_{K^*} \sin^2\theta_l \cos 2\phi + I_4 \sin 2\theta_{K^*} \sin 2\theta_l \cos\phi \\ & + I_5 \sin 2\theta_{K^*} \sin\theta_l \cos\phi \\ & + (I_6^s \sin^2\theta_{K^*} + I_6^c \cos^2\theta_{K^*}) \cos\theta_l + I_7 \sin 2\theta_{K^*} \sin\theta_l \sin\phi \\ & + I_8 \sin 2\theta_{K^*} \sin 2\theta_l \sin\phi + I_9 \sin^2\theta_{K^*} \sin^2\theta_l \sin 2\phi\,. \end{aligned} \tag{3.10}$$

$J_i = I_i$